IN SITU PERMEABILITY ESTIMATION: A COMPARISON BETWEEN ACOUSTIC AND NMR LOGS

Wei Chen and Daniel R. Burns

Earth Resources Laboratory
Department of Earth, Atmospheric, and Planetary Sciences
Massachusetts Institute of Technology
Cambridge, MA 02139

Xiao-ming Tang

Baker Atlas
P.O. Box 1407
Houston, TX 77251

ABSTRACT

Permeability estimates from acoustic logs (Stoneley waves) and NMR logs were compared using data from a geologic section consisting of sandstone and shale beds. The permeability results show very good correlation for these two different methods. Data from a gas-bearing zone shows high permeability values from acoustic data and low values from NMR. The difference between these two permeability results can be used as a gas zone indicator.

INTRODUCTION

Acoustic and Nuclear Magnetic Resonance (NMR) Logging data can been used to estimate *in situ* permeability values. In acoustic logging, as the Stoneley wave propagates past a permeable formation, hydraulic exchange between the wave induced borehole fluid motion and the formation pore fluid system occurs at the borehole wall. This causes a travel time delay and centroid frequency shift in the Stoneley wave relative to propagation in a nonpermeable formation. These changes can be used to estimate permeability (Biot, 1956; Rosenbaum , 1974; Williams *et al.*, 1984; Burns and Cheng, 1986; Winkler *et al.*, 1989, Tang and Cheng, 1993). The advantages of this method are

that the Stoneley wave measurements are directly related to the flow of fluids in the formation, and the logging method is routine. The disadvantages are that the estimates are sensitive to a number of parameters that are not well known, such as the pore fluid compressibility and viscosity as well as the effect of mudcake on the borehole wall.

The NMR logging method is based on the resonance of nuclei in a magnetic field. When subject to a magnetic field, nuclei tend to align their magnetic moments parallel to the field, corresponding to the lowest energy state. The higher the magnetic field, the more nuclei can be polarized and the higher the magnetization of the sample. By transferring energy from electromagnetic fields at specific radio frequencies (RF), the sample magnetization can be turned away from its aligned orientation to a different orientation. The new magnetization generates an RF signal itself, which can be detected. Hydrogen, due to its large magnetic moment and high abundance in water and hydrocarbons, generates a large signal. Thus, the magnitude of the signal is a measure of the fluid-filled porosity in the formation. By measuring the decay or relaxation of the magnetization, information about pore sizes is obtained which can be related to the permeability of the formation. Thus porosity, permeability, and water saturation can be estimated from the NMR logging data. The advantage of this method is that a measure of the pore fluid volume and pore structure is obtained. The disadvantage is that the estimation of permeability is based on simplified Carmen-Kozeny type relationships related to the pore throat sizes obtained from the relaxation times.

This paper presents a comparison between permeability profiles derived from acoustic and NMR logs. A field data set from a sandstone-shale formation is used for the comparison. The effect of a gas zone on the two permeability profiles is also presented.

PERMEABILITY ESTIMATION FROM FULL WAVEFORM ACOUSTIC LOGS

Different borehole acoustic waves are sensitive to different formation properties. The Stoneley wave is especially sensitive to formation permeability. When a Stoneley wave travels along the borehole, this axially symmetric pressure pulse deforms the borehole wall. If the formation is hard, the deformation is small and the propagation velocity is close to the acoustic velocity of the borehole fluid. In a soft formation the deformation is larger resulting in a slower velocity. When the Stoneley wave travels through a permeable formation, it not only deforms the rock matrix but also pushes the pore fluid away from the borehole wall into the formation. As a result, the Stoneley wave velocity decreases and the attenuation increases in a permeable interval. Williams *et al.* (1984) observed such behavior in field data.

Numerical models of borehole wave propagation in porous and permeable media have been developed based on Biot theory (Biot, 1956; Rosenbaum, 1974; Schmitt *et al.*, 1988). Tang *et al.* (1991) developed a simplified Biot-Rosenbaum model, and Tang and Cheng (1993a) developed a one-dimensional approximation for Stoneley wave propagation across permeable zones and fractures that was further expanded to include realistic

borehole irregularities (Tezuka *et al.* 1994) and formation heterogeneities (Gelinsky and Tang, 1997). Based on these developments, a processing methodology has been developed to invert acoustic log data for permeability values (Tang and Cheng, 1996). The method consists of several steps: (1) separate direct transmitted Stoneley waves from reflected waves caused by formation changes and borehole radius changes; (2) model the Stoneley elastic wave propagation effects using formation and borehole parameters from other logs (P and S velocity, density, caliper, mud parameters); (3) comparison between the synthetic and measured wave travel time and attenuation; and (4) permeability estimation from inversion of travel time and attenuation measurements.

Tang *et al.* (1991) showed that the total displacement of a Stoneley wave in a porous and permeable formation could be separated into elastic deformation and fluid flow effects. By comparing the measured Stoneley wave velocity and attenuation to those predicted by the model for a nonporous medium with the same elastic properties, we can separate the effects caused by formation permeability (Burns and Cheng, 1986). This comparison is based on two attributes: the travel time delay and centroid frequency shift. By computing the difference between the computed and predicted travel time delay and centroid frequency shift, we obtain a good indication of formation permeability. For example, if the travel time delay correlates with a centroid frequency shift, one can almost be certain that this phenomenon is due to formation permeability effect.

In order to convert the measured Stoneley wave parameters into permeability values, a calibration point is needed. A reference depth is chosen to provide a source waveform for the synthetic elastic model and to provide a permeability reference value so that permeabilities at other depths can be calculated relative to this reference depth. The reference depth is selected from a relatively homogeneous interval with good caliper and good waveform coherency. The usual approach is to choose a depth in a shale (impermeable) interval and set the permeability value at that depth to zero. By choosing several calibration points, pore fluid parameters (viscosity, density, and bulk modulus) can also be estimated. The pore fluid parameters are difficult to know if multiple fluids are present and the degree of saturation is unknown. In order to estimate these parameters, additional reference depths from intervals with known permeability are chosen. The pore fluid parameters can be estimated based on the known permeabilities and measured Stoneley wave attributes.

PERMEABILITY ESTIMATION FROM NMR LOGS

NMR measurements have long been seen as a means of estimating *in situ* permeability (e.g., Seevers, 1966; Timur, 1969; Chang *et al.,* 1994). Analysis of the relaxation curve from the pulse echo NMR measurements provides a measure of the total fluid filled porosity, the free fluid index (FFI), and the bulk volume irreducible (BVI). FFI is a measure of the moveable fluid in large pores, while BVI is volume of capillary bound fluid contained in small pores (Sklar, 1997). There are two frequently used permeability models. The first is the Coates equation (Timur, 1969) based on the free fluid index

(MFFI):

$$K = c\phi^2 \left(\frac{\mu FFI}{\mu BVI}\right)^2. \quad (1)$$

The second is based on the Carmen-Kozeny relationship and the logarithmic mean of the relaxation time T2 (Morriss *et al.*, 1993):

$$K = c'\phi^4 T_{2L}^2 \quad (2)$$

Both c and c' in these equations are scaling constants. Although some variations of these formulas exist, the general forms of these relations are as shown above.

RESULTS

Comparison Between Acoustic and NMR Log Permeability Estimates

Figures 1a–g show the permeability estimates from Stoneley and NMR data acquired in a sandstone-shale sequence from the North Sea. The first track shows the gamma ray and shear wave slowness. Shear wave slowness is used to build the elastic model, therefore if shear wave data quality is poor the resulting permeability estimates will be unreliable. Track two shows the travel time delay (left) and centroid frequency shift (right) which are used to estimate permeability values. Track three shows the permeability results from acoustic and NMR Logs. The NMR permeability estimate is based on the Coates equation (Timur, 1969). Track four is the measured transmitted Stoneley wave, and track five is the modeled transmitted Stoneley wave without permeability effects. Travel time delay and centroid frequency shift (track two) are calculated from the comparison of these two tracks. Track six shows the measured reflectivity. Track seven shows the modeled reflectivity and the caliper log.

From the results in Figures 1a–g, we see that the permeability calculated from the two different methods (Stoneley wave and NMR) correlate very well. Figure 2 shows a cross-plot of the permeability estimates from the NMR log versus the Stoneley wave log over 130 meters from X060–X190 (an interval of good quality permeability estimates). Although the scatter is significant at very low permeability values (< 0.1 md), most of the values are distributed around the diagonal.

Although the correlation between the two methods is very good for the majority of the section, there are several zones that show significant differences. In Figure 1a, in the interval X740–X758m, the Stoneley permeability is higher than NMR permeability. This difference is due to poor hole conditions as seen on the caliper log in track seven, resulting in unreliable Stoneley permeability values. Another zone (Figure 1e) shows a consistent difference between the Stoneley and NMR permeability estimates. This zone will be discussed in detail in the next section.

Gas Zone Effect on Permeability Estimates

The presence of gas can cause a difference between Stoneley and NMR permeability estimates. The Stoneley wave permeability estimates are calibrated at a reference depth. Using the known permeability value at the reference depth the formation fluid properties are calculated. These fluid properties are then used in estimating permeability values in the remainder of the section. If the fluid properties are not constant, however, the permeability estimates will be in error.

A sensitivity analysis of the modeling parameters shows that the Stoneley wave time delay and frequency shift are primarily controlled by formation permeability, the borehole radius and mud properties, and the pore fluid parameters (viscosity and bulk modulus or incompressibility). Therefore the formation pore fluid viscosity, density and acoustic speed are required to obtain the absolute permeability value. These parameters, however, may be difficult to obtain if multiple fluids exist and the degree of fluid saturation is unknown. Generally, the values of the fluid parameters are representative of water or an oil/water mixture, but not a gas. The result is that in a gas zone, the use of fluid parameter values that are too high will yield a permeability estimate that is too high.

Now we discuss the gas effect on NMR measurements. The phenomenon causing reduced NMR permeability and porosity in gas reservoirs, the so-called "gas effect," is a topic of great interest in the petrophysical community (Flaum *et al.*, 1996). The main reason for the gas effect in NMR measurements is the different relaxation mechanisms between the gas and fluids (brine, oil). Kleinberg and Vinegar (1996) describe the Nuclear Magnetic Resonance relaxation mechanisms in detail.

The transverse relaxation time (T2) of gas may be so short that some or all of the signal from gas may appear in the MBVI window and result in excessively high MBVI values and an estimated porosity value that is too low. Permeability estimates may be very low when using the Coates equation in gas-bearing zones with a gradient-based logging tool. Total NMR porosity will be too low because of the gas effect, while MBVI will be too high and MFFI will be too low, which will result in very low permeability estimation. The Carmen-Kozeny equation will also give erroneous results if used in gas-bearing zone. In this case, the porosity will be too low and the T2L will be smaller than the true T2L because of diffusion, which will yield low estimates of permeability (Akkurt *et al.* 1996).

From the above analysis, when the formation contains gas, permeability estimated from the Stoneley wave will be too high, while permeability estimated from NMR will be too low. This difference could be used as an indication of a gas zone. Density and neutron logs provide a good indication of gas zones. If gas is present, the neutron porosity log (CNL) will show a decrease in porosity due to gas having a lower concentration of hydrogen than water or oil. The formation density (FDC) also measures a lower value (reduced density) in gas zones. If we plot these logs with scales in opposite directions, the separation between the two values is a good indication of gas. Figure 3 shows the FDC-CNL separation for the interval from X040–X060 m where the difference was ob-

served between Stoneley and NMR permeability estimates. The FDC-CNL separation indicates the presence of gas in this sandstone interval, a result consistent with the permeability estimates. Based on this analysis, we conclude that the disagreement between Stoneley and NMR permeability estimates in this interval is due to the presence of gas.

CONCLUSIONS

Logging data from a shale-sand sequence was used to compare permeability estimates from acoustic and NMR log. The results correlate very well. A gas zone effect on permeability estimation from Stoneley waves and NMR was also analyzed. The presence of gas in the formation, however, causes permeability values estimated from Stoneley wave data to be too high, and permeability values estimated from NMR data to be too low. The difference between these two curves can be used as a gas zone indicator.

ACKNOWLEDGMENTS

This work was supported by the Borehole Acoustics and Logging/Reservoir Delineation Consortia at the Massachusetts Institute of Technology.

REFERENCES

Akkurt, R., Vinegar, H.J., Tutunjian, P.N., Guillory, and A.J., 1996, NMR logging of natural gas reservoirs, *The Log Analyst, 37,* 33–42.

Biot, M., 1956, Theory of propagation of elastic waves in a fluid-saturated porous solid, *J. Acoust. Soc. Am.,* 168–191.

Burns, D.R., and Cheng, C.H., 1986, Determination of in situ permeability from tube wave velocity and attenuation, *Trans. SPWLA, 27th Ann. Logging Symp., Paper LL.*

Chang, D., Vinegar, H., Morriss, C., and Straly, C., 1994, Effective porosity, producible fluid and permeability in carbonates from NMR logging, presented at the 35th Annual Logging Symposium, SPWLA.

Flaum, C., Kleinberg, R.L., and Hürliman, M.D., 1996, Identification of gas with the combinable magnetic resonance tool (CMR), presented at the 37th Annual Logging Symposium, SPWLA, Paper L.

Gelinsky, S., and Tang, X.M., 1997, Modeling of Stoneley waves in a heterogeneous formation with an irregular borehole, presented at 59th EAEG conference, Geneva, Switzerland.

Kleinberg, R.L., and Vinegar, H.J., 1996, NMR properties of reservoir fluids, *The Log Analyst, 37,* 20–32.

Morriss, C.E., Macinnis, J., Freedman, R., Smaardyk, J., Straley, C., Kenyon, W.E., Vinegar, H.J., and Tutunjian, P.N., 1993, Field test of an experimental pulsed nuclear magnetism tool, presented at 34th Annual Logging Symposium, SPWLA, Paper GGG.

Rosenbaum, J.H., 1974, Synthetic microsesmograms: logging in porous formations, *Geophysics, 39,* 14–32.

Seevers, D.O., 1966, A nuclear magnetic method for determining the permeability of sandstone, presented at Annual Logging Symposium Transaction, SPWLA, Paper L.

Sklar, H.F., 1997, Nuclear magnetic resonance kogging, M.S. Thesis, MIT.

Tang, X.M., Cheng, C.H., and Toksöz, M.N., 1991, Dynamic permeability and borehole Stoneley waves: A simplified Biot-Rosenbaum Model, *J. Acoust. Soc. Am., 90,* 1632–1644.

Tang, X.M. and Cheng, C.H., 1993a, Boreholes Stoneley wave propagation across permeable structures, *Geophys. Prosp., 41,* 165–187.

Tang, X.M., and Cheng, C.H., 1993b, Effects of a logging tool on the Stoneley waves in elastic and porous boreholes, *The Log Analyst, 34,* 46–56.

Tang, X.M., Cheng C.H., 1996, Fast inversion of formation permeability from Stoneley wave log using a simplified Biot-Rosenbaum model, *Geophysics, 61,* 639–645.

Tezuka, K., Cheng, C.H., and Tang, X.M., 1994, Modeling of low-frequency Stoneley wave propagation in an irregular borehole, *Expand. Abstracts, 64th SEG Annual Mtg.,* Los Angeles, CA, 24–27.

Timur, A., 1969, Pulsed nuclear magnetic resonance studies of porosity, moveable fluid, and permeability of sandstones, *J. Petroleum Technology, 21,* 775–786.

Schmitt, D.P., Bouchon, M., and Bonnet, G., 1988, Full-wave synthetic acoustic logs in radially semi-infinite saturated porous media , *Geophysics, 53,* 807–823.

Williams, D.M., Zemanek, J., Angona, F.A., Dennis, C.L, and Caldwell, R.L., 1984, The long spaced acoustic logging tool, presented at 25th Annual Logging Symposium, SPWLA, Paper T.

Winkler, K.W., Liu, H.L., and Johnson, D.L., 1989, Permeability and borehole Stoneley waves: Comparison between experiment and theory, *Geophysics, 52,* 66–75.

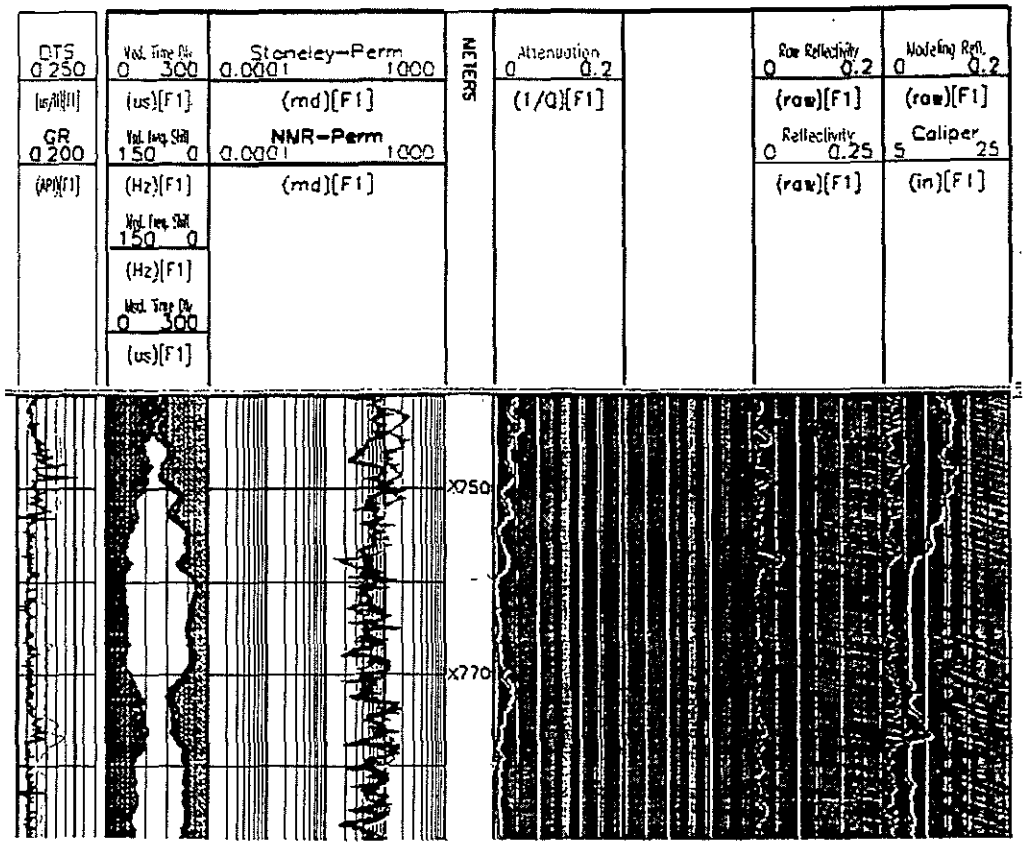

Figure 1a: Permeability results from X750-X780m with bad caliper. First track shows GR (black), shear wave slowness (red). Track two shows centroid frequency shift (blue) and travel time delay (red). Track three shows the permeability estimated from Stoneley wave (red) and permeability estimated from NMR (blue). Track four shows the attenuation and measured Stoneley wave. Track five shows the modeled Stoneley wave. Track six shows the reflectivity and measured reflection. Track seven shows the caliper and modeled reflection.

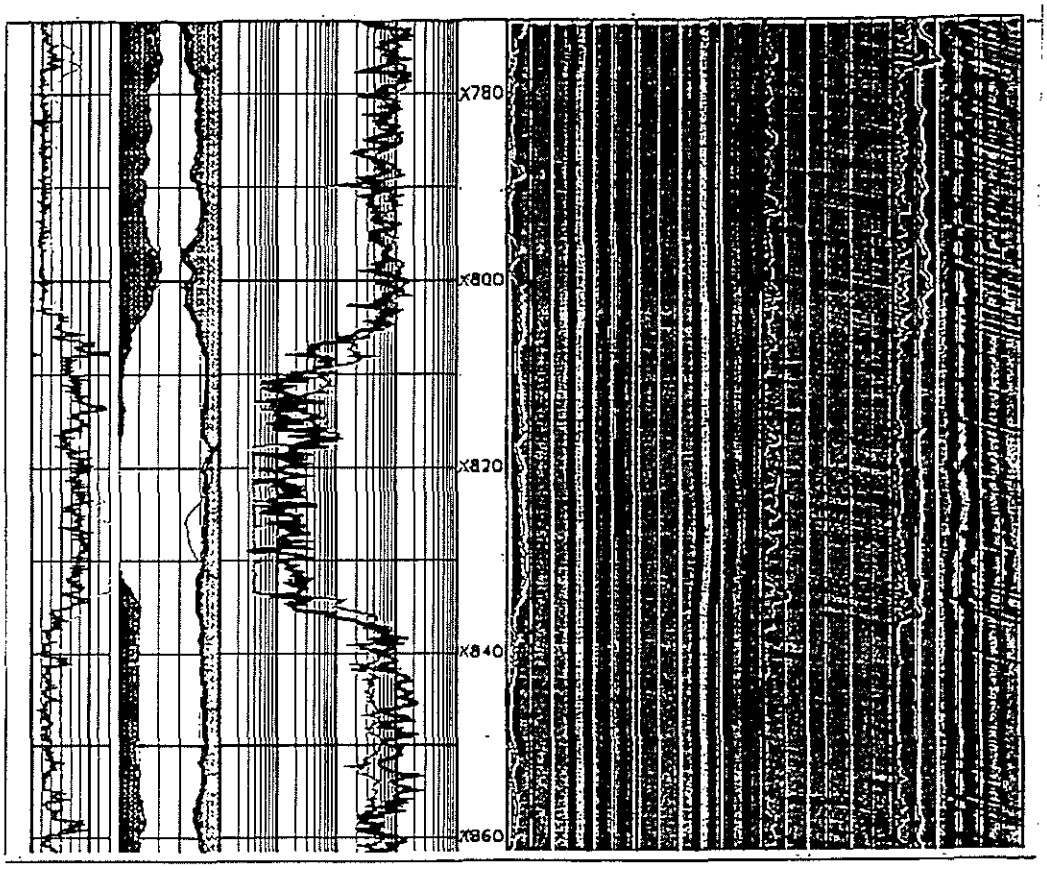

Figure 1b: Permeability results from interval X780-X860m. A shale formation is indicated by GR, the permeability values in this shale formation are low.

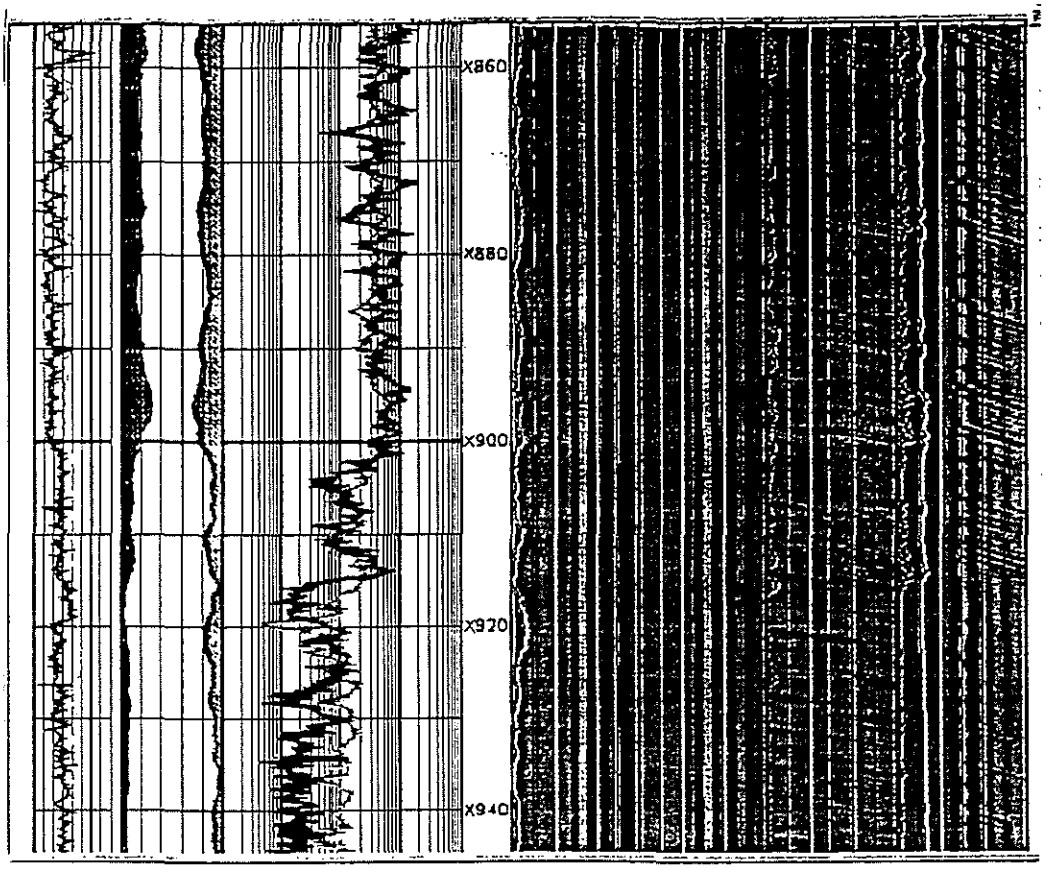

Figure 1c: Permeability results from X860-X940m. Good correlation is observed from this interval.

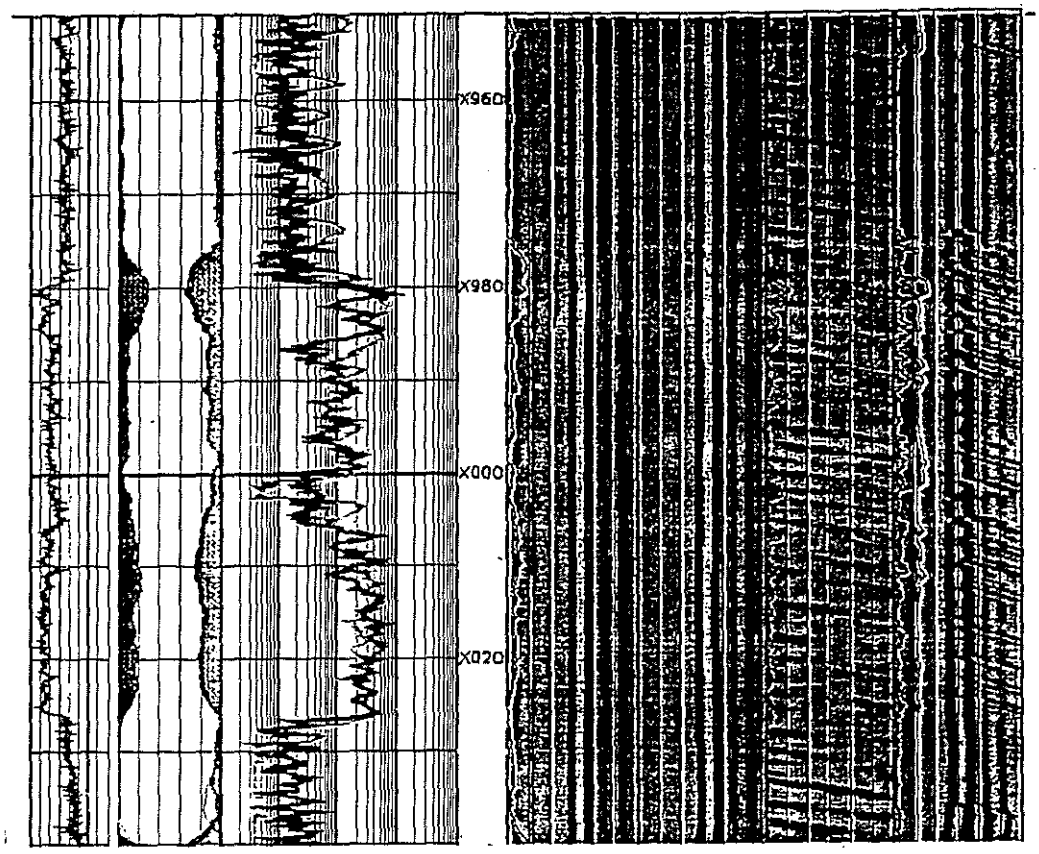

Figure 1d: Permeability results from X960-X030.

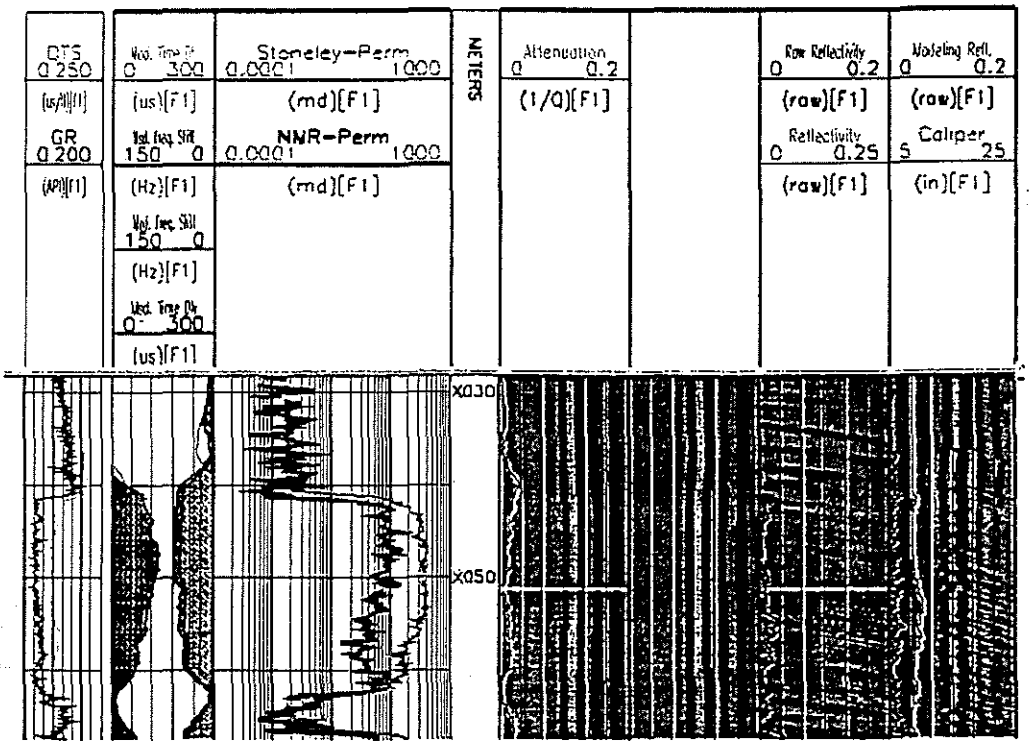

Figure 1e: Permeability results from interval X030-X070m. Permeability difference is observed.

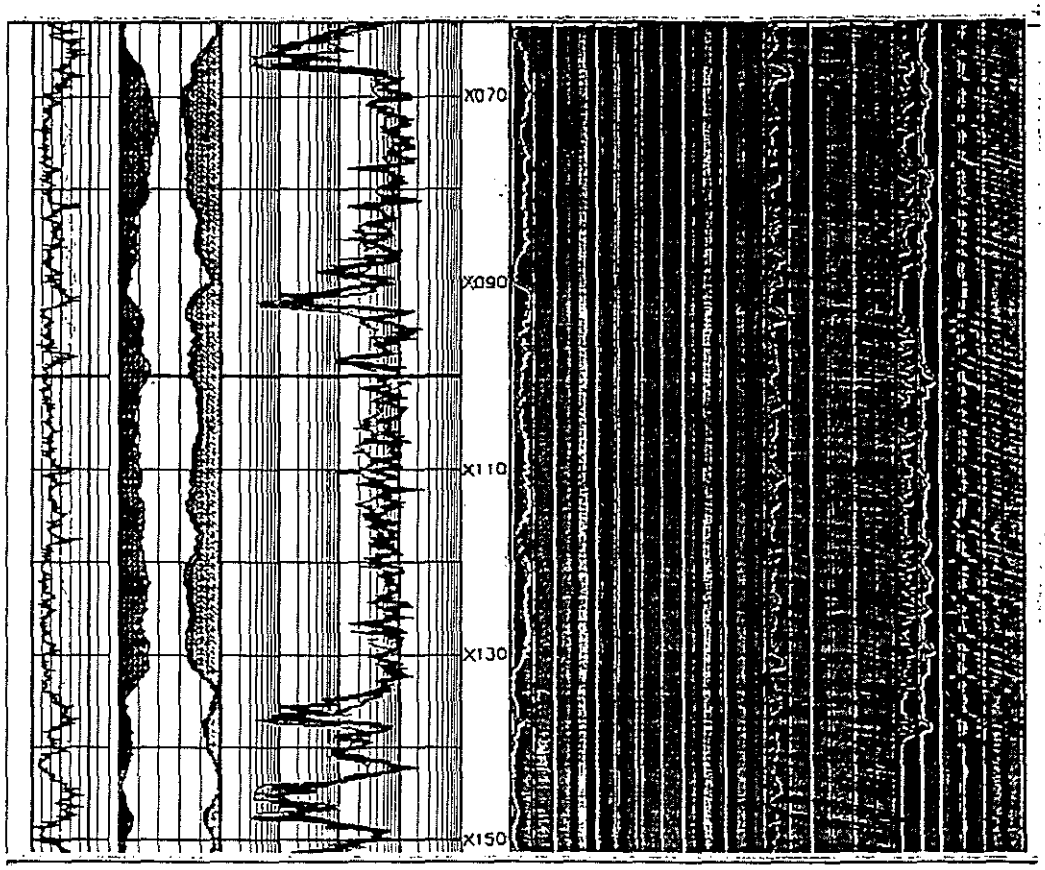

Figure 1f: Permeability results from interval X070-X150. It is one of the continuous intervals in a whole well profile.

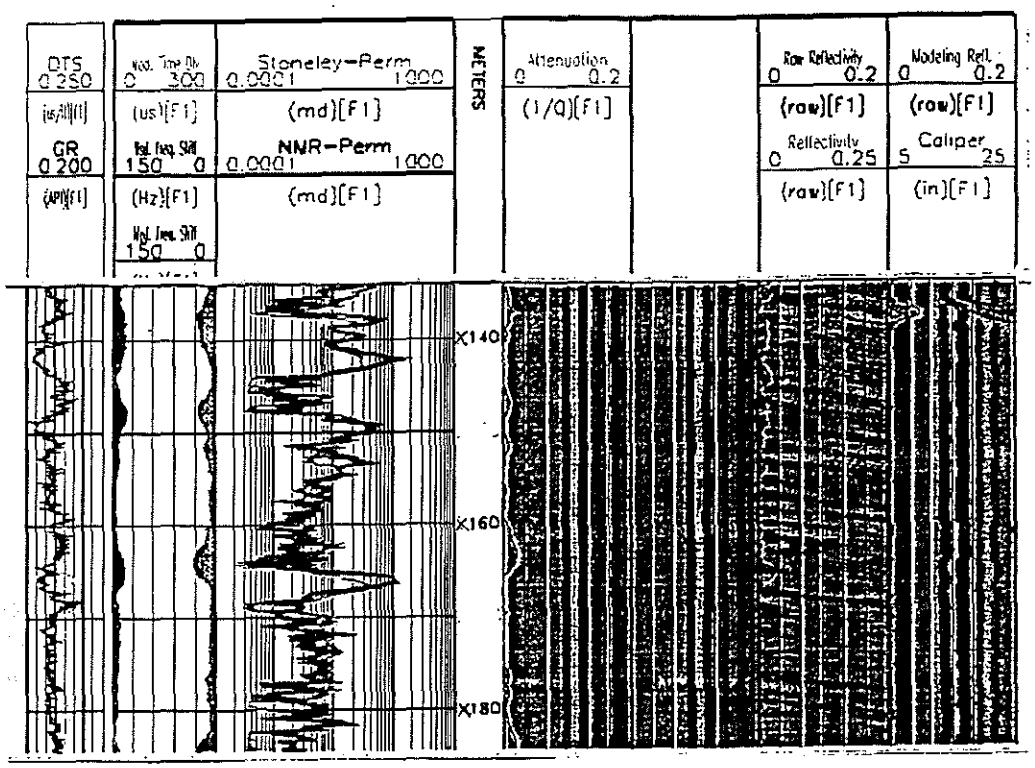

Figure 1g: Permeability results from X140-X180m (bottom part of the whole well).

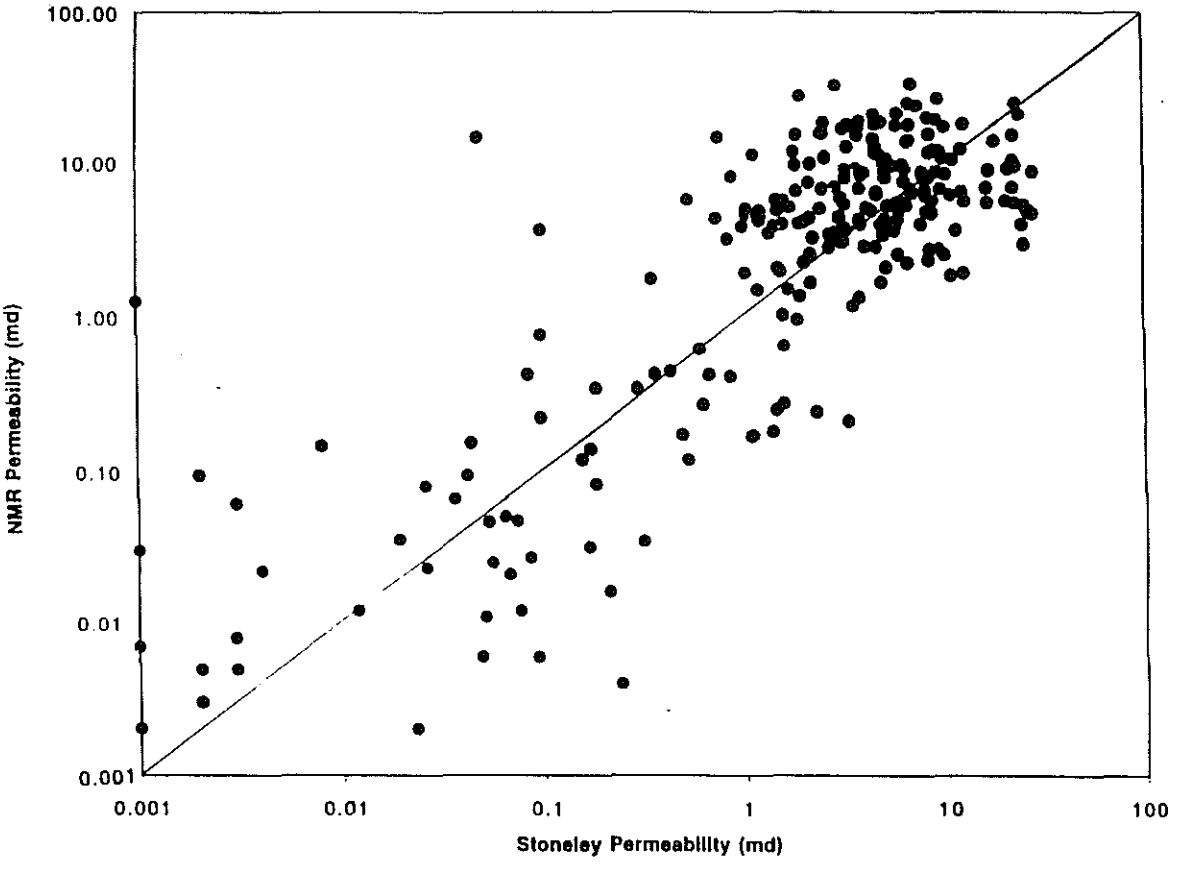

Figure 2: Crossplot of NMR and Stoneley wave permeability estimates.

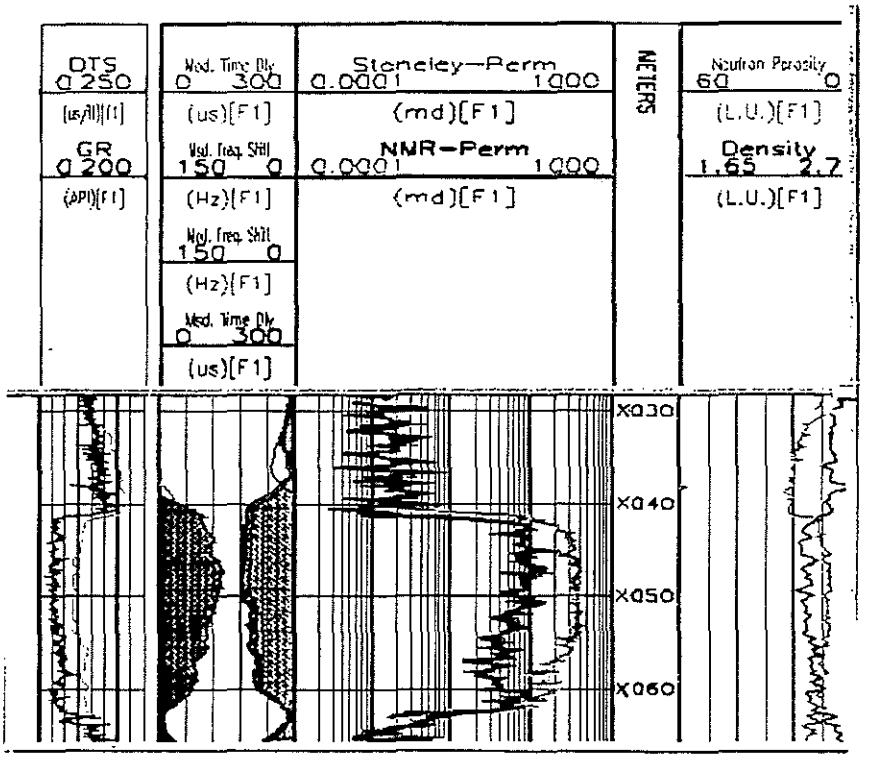

Figure 3: FDC-CNL gas zone indication (track four).